Supporting Information

Furutani et al. 10.1073/pnas.1316109111

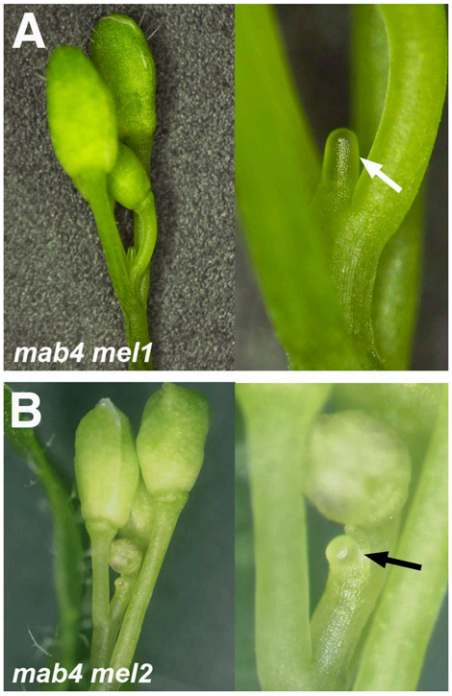

Fig. S1. Mutation of *mel1* and *mel2* enhances the *mab4* phenotypes. (*A* and *B*) Inflorescences of *mab4-2 mel1-1* (*A*) and *mab4-2 mel2-1* double mutants (*B*). The right panel of *A* and *B* shows a magnified image around the inflorescence meristem, respectively. The arrows indicate pin-shaped inflorescences.

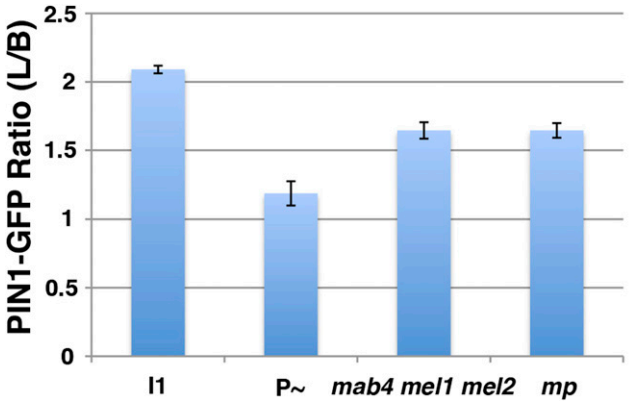

Fig. S2. The ratio of PIN1-GFP intensity on lateral side to that on bottom side of plasma membrane of epidermis. The graph displays the ratio of intensity of PIN1-GFP fluorescence on lateral side to that on bottom side of epidermis around the convergence points of PIN1-GFP in wild-type immature primordia (I1) and developing primordia (P~), *mab4-2 mel1-1 mel2-1*, and *mp-T370* (N_{I1} = 14, $N_{P\sim}$ = 12, $N_{mab4\ mel1\ mel2}$ = 12, N_{mp} = 12). Error bars represent SEM.

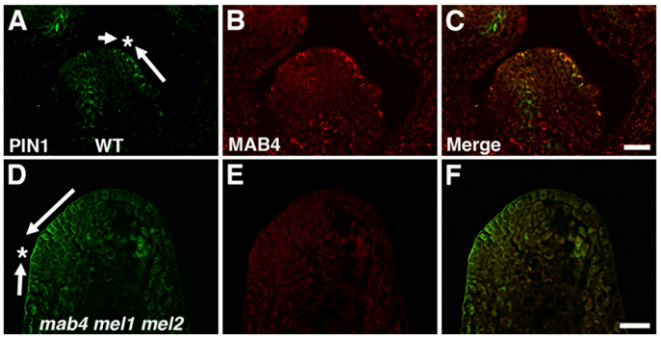

Fig. S3. PIN1 and MAB4 localization in *mab4-2 mel1-1 mel2-1* triple mutants. (*A*–*C*) Immunolocalization of PIN1 (*A*) and MAB4 (*B*) in the wild-type inflorescence meristem. Cells colabeled with PIN1 (green) and MAB4 (red) are seen as yellow signals in the merged image (*C*). The arrows indicate predicted polar auxin transport. The asterisk indicates a convergence point of PIN1 polarity. (*D*–*F*) PIN1 (*D*) and MAB4 (*E*) localization in a *mab4-2 mel1-1 mel2-1* inflorescence. Merged image of PIN1 (green) and MAB4 (red) staining (*F*). (Scale bars: 20 μm.)

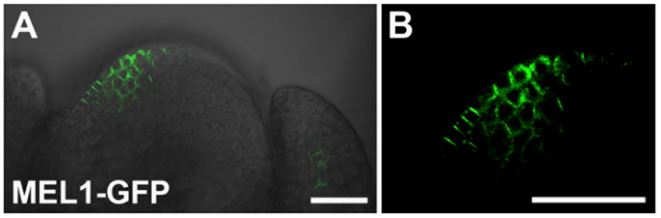

Fig. S4. MEL1-GFP localization in the inflorescence meristem. (*A* and *B*) GFP fluorescence images of MEL1-GFP, merged with the Nomarski image (*A*) and magnified at the peripheral region of the meristem (*B*). (Scale bars: 20 μm.)

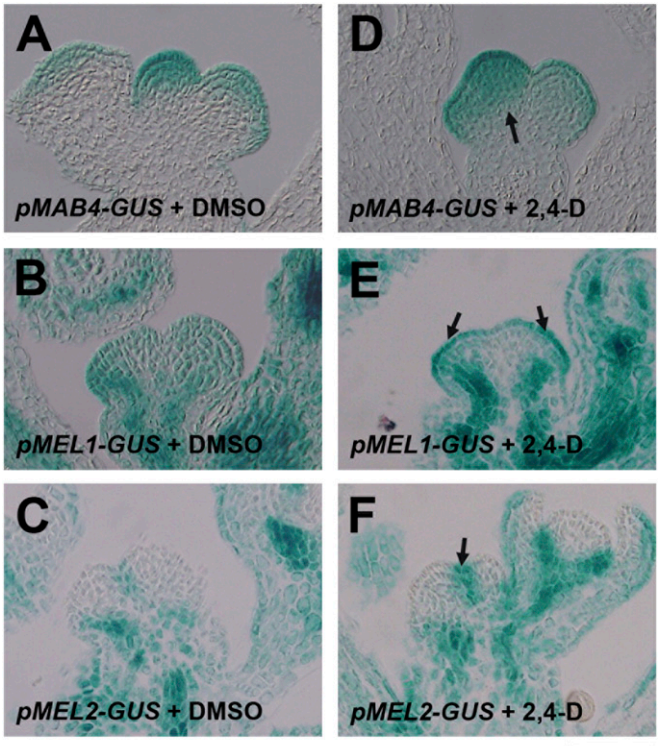

Fig. S5. Auxin treatment up-regulated expression of the *MAB4* family genes. (*A*–*F*) GUS staining of *pMAB4::GUS* (*A* and *D*), *pMEL1::GUS* (*B* and *E*), and *pMEL2::GUS* (*C* and *F*) in inflorescences, treated with DMSO (*A*–*C*) and 10 μM the synthetic auxin 2,4-dichlorophenoxyacetic acid (2,4-D) (*D*–*F*) for 6 h, respectively. The arrows in *D*–*F* show increased GUS staining. [Scale bar: 100 μm (for *A*–*F*)].

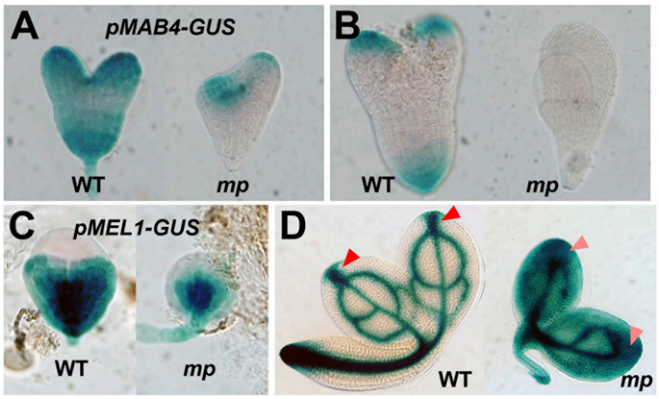

Fig. S6. Decreased expression of the *MAB4* family genes in *mp* embryos. (*A* and *B*) GUS staining of *pMAB4::GUS* in the wild-type (*Left*) and *mp-T370* (*Right*) embryos at the heart (*A*) and torpedo stage (*B*). (*C* and *D*) GUS staining of *pMEL1::GUS* in the wild-type (*Left*) and *mp-T370* (*Right*) embryos at the heart (*C*) and mature stage (*D*). The red arrowheads in *D* indicate GUS activity at the tips of cotyledon. Strong GUS staining was detected in wild type (*Left*), but reduced GUS staining was found in *mp-T370* (*Right*).

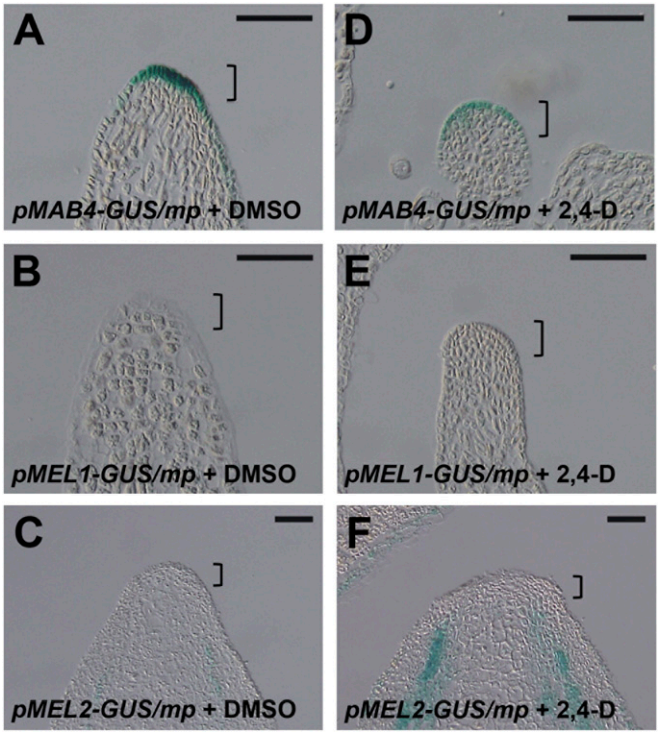

Fig. S7. No effect of auxin treatment on the *MAB4* family gene expression in *mp* inflorescences. (*A*–*F*) GUS staining of *pMAB4::GUS* (*A* and *D*), *pMEL1::GUS* (*B* and *E*), and *pMEL2::GUS* (*C* and *F*) in *mp-T370* inflorescences, treated with DMSO (*A*–*C*) and 10 μM 2,4-D (*D*–*F*) for 6 h, respectively. The brackets in *A*–*F* show meristem area. (Scale bars: 100 μm.)

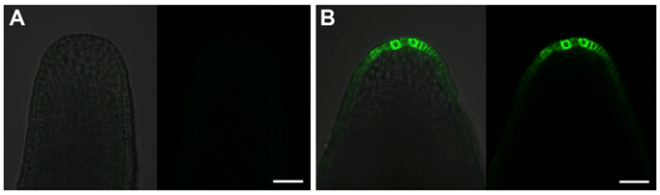

Fig. S8. *DR5rev::GFP* expression in *mp* inflorescences. (*A* and *B*) *DR5rev::GFP* expression in pin-shaped inflorescences of *mp-T370*. GFP fluorescence images (*Right*) and merged images with Nomarski images (*Left*). Many of mutant meristem displayed no GFP signal (*A*). GFP signal was occasionally found in the L1 layer of the mutant apex (*B*). (Scale bars: 20 μm.)